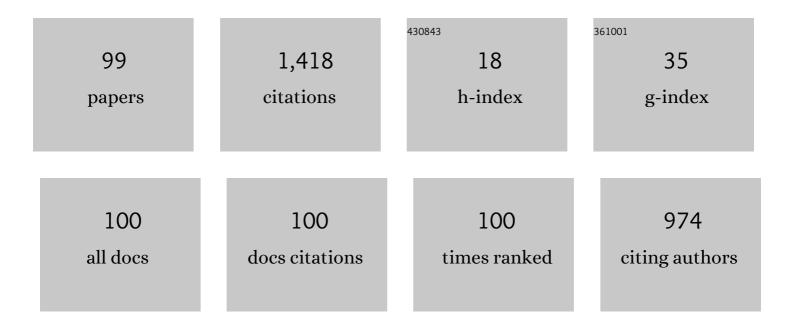
List of Publications by Year in descending order

Source: https://exaly.com/author-pdf/8267099/publications.pdf Version: 2024-02-01



#	Article	IF	CITATIONS
1	β-Gallium oxide power electronics. APL Materials, 2022, 10, .	5.1	184
2	Detection of acceptor-bound exciton peak at 300ÂK in boron–phosphorus co-doped ZnMgO thin films for room-temperature optoelectronics applications. Optical Materials, 2021, 111, 110591.	3.6	4
3	Detailed investigation of MOCVD-grown [beta]-Ga2O3 through quantitative defect spectroscopies. , 2021, , .		2
4	Realization of high-quality RF sputtered ZnMgO (x=15%) thin films by post-growth annealing treatment. Superlattices and Microstructures, 2021, 156, 106977.	3.1	5
5	Enhancement in structural, elemental and optical properties of boron–phosphorus Co-doped ZnO thin films by high-temperature annealing. Journal of Luminescence, 2021, 238, 118221.	3.1	8
6	Electrostatic Engineering Using Extreme Permittivity Materials for Ultra-Wide Bandgap Semiconductor Transistors. IEEE Transactions on Electron Devices, 2021, 68, 29-35.	3.0	30
7	Enhancing responsivity and detectivity in broadband UV–VIS photodetector by ex-situ UV–ozone annealing technique. Superlattices and Microstructures, 2020, 137, 106333.	3.1	15
8	Influence of growth temperature on defect states throughout the bandgap of MOCVD-grown <i>β</i> -Ga2O3. Applied Physics Letters, 2020, 117, .	3.3	21
9	Room-temperature ultraviolet-ozone annealing of ZnO and ZnMgO nanorods to attain enhanced optical properties. Journal of Materials Science: Materials in Electronics, 2020, 31, 18777-18790.	2.2	4
10	High electron density <i>β</i> -(Al0.17Ga0.83)2O3/Ga2O3 modulation doping using an ultra-thin (1 nm) spacer layer. Journal of Applied Physics, 2020, 127, .	2.5	64
11	Probing Charge Transport and Background Doping in Metalâ€Organic Chemical Vapor Depositionâ€Grown (010) βâ€Ga ₂ O ₃ . Physica Status Solidi - Rapid Research Letters, 2020, 14, 2000145.	2.4	79
12	Full bandgap defect state characterization of <i>β</i> -Ga2O3 grown by metal organic chemical vapor deposition. APL Materials, 2020, 8, .	5.1	52
13	Zinc Magnesium Oxide-Based Nanorods for High-Precision pH Sensing. IEEE Sensors Journal, 2020, 20, 4587-4594.	4.7	2
14	Improving optical properties and controlling defect-bound states in ZnMgO thin films through ultraviolet–ozone annealing. Thin Solid Films, 2020, 708, 138112.	1.8	7
15	Effect of UV-Ozone annealing on the transient characteristics of ZnMgO thin film UV-Vis photodetector. , 2020, , .		0
16	Electrical Properties 3. Springer Series in Materials Science, 2020, , 421-441.	0.6	0
17	Bipolar Analog Memristive Switching of In ₂ O ₃ Using Al Nanoparticles. Journal of Nanoscience and Nanotechnology, 2019, 19, 8126-8134.	0.9	5
18	Mechanism of Si doping in plasma assisted MBE growth of \hat{I}^2 -Ga2O3. Applied Physics Letters, 2019, 115, .	3.3	41

#	Article	IF	CITATIONS
19	Detailed investigation of photoluminescence, structural, and elemental properties of ZnO thin films under various annealing ambient. Superlattices and Microstructures, 2019, 136, 106310.	3.1	14
20	Unusual Formation of Point-Defect Complexes in the Ultrawide-Band-Gap Semiconductor <mml:math xmlns:mml="http://www.w3.org/1998/Math/MathML" display="inline"><mml:mrow><mml:mi>β</mml:mi><mml:mtext>â^`</mml:mtext><mml:msub><mml:mrow>< mathvariant="normal">O</mml:mrow><mml:mrow><mml:mn>3</mml:mn></mml:mrow>Physical Review X, 2019, 9, .</mml:msub></mml:mrow></mml:math 		
21	InN Nanowires Based Near-Infrared Broadband Optical Detector. IEEE Photonics Technology Letters, 2019, 31, 1526-1529.	2.5	7
22	Impact of deep level defects induced by high energy neutron radiation in β-Ga2O3. APL Materials, 2019, 7,	5.1	80
23	High performance short wave infrared photodetector using p-i-p quantum dots (InAs/GaAs) validated with theoretically simulated model. Journal of Alloys and Compounds, 2019, 804, 18-26.	5.5	10
24	<i>In situ</i> measurement of temperature dependent picosecond resolved carrier dynamics in near infrared (NIR) sensitive device on action. Review of Scientific Instruments, 2019, 90, 043909.	1.3	5
25	Monitoring soil pH variation using Polyaniline/SU-8 composite film based conductometric microsensor. Sensors and Actuators B: Chemical, 2019, 286, 583-590.	7.8	27
26	Enhancing Acceptor-Based Optical Behavior in Phosphorus-Doped ZnO Thin Films Using Boron as Compensating Species. ACS Applied Electronic Materials, 2019, 1, 325-339.	4.3	6
27	Influence of neutron irradiation on deep levels in Ge-doped (010) \hat{l}^2 -Ga2O3 layers grown by plasma-assisted molecular beam epitaxy. APL Materials, 2019, 7, .	5.1	31
28	Inversion of activity in DSSC for TiO2 and ZnO photo-anodes depending on the choice of sensitizer and carrier dynamics. Journal of Luminescence, 2019, 207, 169-176.	3.1	17
29	Enhanced optical properties with the assimilation of boron and phosphorus dopant in co-doped ZnO thin film. , 2019, , .		Ο
30	Impact of ternary capping on p-i-p InAs/GaAs quantum-dot infrared photodetectors. , 2019, , .		0
31	Investigating time-varying phosphorous doping effect on the structural and optical properties of ZnO thin films. , 2019, , .		0
32	Influence of modulation doping on p-i-p quantum-dots (InAs/GaAs)-based infrared detector performance. , 2019, , .		0
33	Enhancement of photocurrent and responsivity of Zn1-xMgxO (x=15%)-based ultraviolet detector by UV-ozone treatment. , 2019, , .		Ο
34	Impact of ultra-thin quaternary capping on modulation doped p-i-p quantum dots (InAs/GaAs) based infrared detector. , 2019, , .		0
35	Interdependence of Ar and O2 partial pressure on the properties of RF sputtered Zn0.85Mg0.15O thin film. , 2019, , .		Ο
36	Improvement in performance characteristics of Zn(1-x)MgxO (x=15%) thin film transistor (TFT) with UV-ozone treatment. , 2019, , .		0

#	Article	IF	CITATIONS
37	Augmenting optical and structural properties in Zn0.85Mg0.15O thin film with P-B co-doping. , 2019, , .		Ο
38	Enhancement in optical properties with suppression of defect states by UV-ozone processing in RF sputtered Zn(1-x)MgxO (x=15%) thin film. , 2019, , .		0
39	Improvement in operating temperature of InAs/GaAs quantum-dots-based photodetectors by varying position of localized carriers in active region. , 2019, , .		0
40	Enhancement in optical properties of ZnO nanorods by UV ozone treatment. , 2019, , .		1
41	Time dependent boron implantation effect on the dopant solubility and optical properties of phosphorus doped ZnO thin films. , 2019, , .		0
42	Role of Pzn-2Vzn centre on the luminescence properties of phosphorus doped ZnO thin films by varying doping concentration. Journal of Luminescence, 2018, 200, 120-125.	3.1	17
43	Optimizing dot-in-a-well infrared detector architecture for achieving high optical and device efficiency corroborated with theoretically simulated model. Journal of Alloys and Compounds, 2018, 751, 337-348.	5.5	7
44	Improved Absorbance and Near-Infrared Dispersion of AuGe Nanoparticles over Au Nanoparticles Prepared with Similar Thermal Annealing Environment. Plasmonics, 2018, 13, 1947-1962.	3.4	4
45	Boosted UV Sensitivity of Er-Doped In2O3 Thin Films Using Plasmonic Ag Nanoparticle-Based Surface Texturing. Plasmonics, 2018, 13, 1105-1113.	3.4	13
46	Deep level defects in Ge-doped (010) β-Ga2O3 layers grown by plasma-assisted molecular beam epitaxy. Journal of Applied Physics, 2018, 123, .	2.5	91
47	Emerging material zinc magnesium oxide based nanorods: Growth process optimization and sensor application towards humidity detection. Sensors and Actuators B: Chemical, 2018, 256, 204-216.	7.8	31
48	Ultrasensitive zinc magnesium oxide nanorods based micro-sensor platform for UV detection and light trapping. Sensors and Actuators A: Physical, 2018, 278, 127-139.	4.1	13
49	Oblique angle deposited InN quantum dots array for infrared detection. Journal of Alloys and Compounds, 2018, 766, 297-304.	5.5	11
50	Effects of phosphorus implantation time on the optical, structural, and elemental properties of ZnO thin films and its correlation with the 3.31-eV peak. Journal of Alloys and Compounds, 2018, 768, 800-809.	5.5	18
51	Trapping Effects in Si -Doped -Ga ₂ O ₃ MESFETs on an Fe-Doped -Ga ₂ O ₃ Substrate. IEEE Electron Device Letters, 2018, 39, 1042-1045.	3.9	78
52	Co-relation of theoretical simulation with experimental results for InAs quantum-dot heterostructures with different capping material. , 2018, , .		0
53	Highly efficient InAs/InGaAs quantum dot-in-a-well heterostructure validated with theoretically simulated model. , 2018, , .		0
54	Effect of time varying phosphorus implantation on optoelectronics properties of RF sputtered ZnO thin-films. , 2018, , .		0

#	Article	IF	CITATIONS
55	Temperature-dependent phosphorous dopant activation in ZnO thin film deposited using plasma immersion ion implantation. , 2018, , .		Ο
56	Short wave infrared photodetector using p-i-p quantum dots (InAs/GaAs) for high temperature operation. , 2018, , .		0
57	Modelling of dark current and noise dependence on capping thickness in quantum dots based infrared photodetectors. , 2018, , .		0
58	Ultranarrow spectral response of InGaAs QDIPs through the optimization of strain-coupled stacks and capping layer composition. Materials Science in Semiconductor Processing, 2017, 60, 40-44.	4.0	28
59	Photo-induced electronic properties in single quantum well system: effect of excitonic lifetime. Materials Research Express, 2017, 4, 016301.	1.6	6
60	Improvement in grain size and crystallinity of sputtered ZnO thin film with optimized annealing ambient. , 2017, , .		0
61	Enhancement of photoluminescence in RF sputtered ZnMgO thin films by optimizing annealing temperature. Proceedings of SPIE, 2017, , .	0.8	Ο
62	Utilization of self-assembled AuGe nanoparticles for improving performance of InGaAs/GaAs quantum dot infrared detector. Journal of Materials Science: Materials in Electronics, 2017, 28, 12497-12502.	2.2	3
63	Confinement Barrier Induced Enhancement in Thermal Stability of the Optical Response of InAs/InGaAs/GaAs Submonolayer Quantum Dot Heterostuctures. MRS Advances, 2017, 2, 2349-2354.	0.9	2
64	Design and Fabrication of 320Â×Â256 Focal-Plane Array Using Strain-Coupled Quaternary Capped InAs/GaAs Quantum Dots Infrared Photo-Detectors for Thermal Imaging. Lecture Notes in Electrical Engineering, 2017, , 93-99.	0.4	1
65	Enhancement in optical characteristics of c-axis-oriented radio frequency–sputtered ZnO thin films through growth ambient and annealing temperature optimization. Materials Science in Semiconductor Processing, 2017, 66, 1-8.	4.0	33
66	Minimization of material inter-diffusion for thermally stable quaternary-capped InAs quantum dot via strain modification. Superlattices and Microstructures, 2017, 105, 117-131.	3.1	13
67	Evidence of quantum dot size uniformity in strain-coupled multilayered In(Ga)As/GaAs QDs grown with constant overgrowth percentage. Journal of Luminescence, 2017, 192, 562-566.	3.1	17
68	The impact of confinement enhancement AlGaAs barrier on the optical and structural properties of InAs/InGaAs/GaAs submonolayer quantum dot heterostructures. Journal of Luminescence, 2017, 192, 277-282.	3.1	13
69	Pine shaped InN nanostructure growth via vapour transport method by own shadowing and infrared detection. Journal of Alloys and Compounds, 2017, 722, 872-877.	5.5	9
70	Indigenous Development of 320 x 256 Focal-Plane Array Using InAs/InGaAs/GaAs Quantum Dots-In-A-Well Infrared Detectors for Thermal Imaging. Current Science, 2017, 112, 1568.	0.8	15
71	AuGe surface plasmon enhances photoluminescence of the InAs/GaAs bilayer quantum dot heterostructure. RSC Advances, 2016, 6, 26908-26913.	3.6	8
72	Increasing peak detectivity (D*) of In _{0.5} Ga _{0.5} As/GaAs quantum dot infrared photodetectors by up to two orders with highâ€energy proton implantation. Electronics Letters, 2016, 52, 61-63.	1.0	2

#	Article	IF	CITATIONS
73	Enhancement in multicolor photoresponse for quaternary capped In0.5Ga0.5As/GaAs quantum dot infrared photodetectors implanted with hydrogen ions. Materials Research Bulletin, 2016, 84, 79-84.	5.2	8
74	Growth technique and effect of post growth annealing on the optical properties of In(Ga)As/GaAs quantum dot heterostructures. Proceedings of SPIE, 2016, , .	0.8	0
75	Enhancement in device performance of hepta-layer coupled InGaAs quantum dot infrared detector by AuGe surface plasmons. , 2016, , .		0
76	A detailed investigation of the impact of varying number of dot layers in strain-coupled multistacked InAs/GaAs quantum dot heterostructures. Proceedings of SPIE, 2016, , .	0.8	0
77	Effect of varying capping composition and number of strain-coupled stacks on In0.5Ga0.5As quantum dot infrared photodetectors. , 2016, , .		0
78	Enhancement in optical and structural properties of Zn _{0.85} Mg _{0.15} O nanorods over thin films synthesized by hydrothermal chemical treatment. Proceedings of SPIE, 2016, ,	0.8	0
79	Optimization of the Number of Stacks in the Submonolayer Quantum Dot Heterostructure for Infrared Photodetectors. IEEE Nanotechnology Magazine, 2016, 15, 214-219.	2.0	17
80	Comparison of Three Design Architectures for Quantum Dot Infrared Photodetectors: InGaAs-Capped Dots, Dots-in-a-Well, and Submonolayer Quantum Dots. IEEE Nanotechnology Magazine, 2015, 14, 603-607.	2.0	11
81	Enhancement of device performance by using quaternary capping over ternary capping in strain-coupled InAs/GaAs quantum dot infrared photodetectors. Applied Physics A: Materials Science and Processing, 2015, 118, 511-517.	2.3	16
82	Effects of high energy proton implantation on the optical and electrical properties of In(Ga)as/GaAs QD heterostructures with variations in the capping layer. Journal of Luminescence, 2015, 161, 129-134.	3.1	4
83	Stability in peak emission wavelength in strain-coupled multilayer InAs/GaAs quantum dot heterostructures when subjected to high-temperature rapid thermal annealing. , 2015, , .		0
84	Cross-sectional TEM (XTEM) analysis for vertically coupled quaternary In0.21Al0.21Ga0.58As capped InAs/GaAs quantum dot infrared photodetectors. , 2015, , .		1
85	Enhancement in Peak Detectivity and Operating Temperature of Strain-Coupled InAs/GaAs Quantum Dot Infrared Photodetectors by Rapid Thermal Annealing. IEEE Nanotechnology Magazine, 2015, 14, 668-672.	2.0	5
86	A detail investigation on quaternary and ternary capped strain coupled quantum dots based infrared photodetectors and effect of rapid thermal annealing temperature. , 2015, , .		1
87	Effect of high energy proton implantation on the device characteristics of InAlGaAs-capped InGaAs/GaAs quantum dot based infrared photodetectors. Proceedings of SPIE, 2015, , .	0.8	0
88	The optical properties of strain-coupled InAs/GaAs quantum-dot heterostructures with varying thicknesses of GaAs and InGaAs spacer layers. Journal of Luminescence, 2015, 158, 231-235.	3.1	23
89	A detailed study of the effects of rapid thermal annealing on the luminescence properties of InAs sub-monolayer quantum dots. Journal of Luminescence, 2015, 158, 149-152.	3.1	27
90	Direct Determination of Energy Band Alignments of Ni/Al2O3/GaN MOS Structures Using Internal Photoemission Spectroscopy. Journal of Electronic Materials, 2014, 43, 828-832.	2.2	16

#	Article	IF	CITATIONS
91	Tuning in spectral response due to rapid thermal annealing on dot-in-a-well infrared photodetectors. Superlattices and Microstructures, 2014, 65, 106-112.	3.1	11
92	Effect of barrier thickness on structural, optical, and spectral behaviors of vertically strain coupled InAs/GaAs quantum dot infrared photodetectors. Journal of Vacuum Science and Technology B:Nanotechnology and Microelectronics, 2014, 32, .	1.2	10
93	One order enhancement of detectivity in quaternary capped InAs/GaAs quantum dot infrared photodetectors due to vertical coupling of quantum dot layers. Thin Solid Films, 2014, 566, 1-4.	1.8	19
94	Reduction of dark current density by five orders at high bias and enhanced multicolour photo response at low bias for quaternary alloy capped InGaAs/ GaAs QDIPs, when implanted with low-energy light (H-) ions. Proceedings of SPIE, 2013, , .	0.8	0
95	Influence of low energy H-ion implantation on the electrical and material properties of quaternary alloy (In0.21Al0.21Ga0.58As) capped InAs/GaAs n-i-n QDIPs. , 2013, , .		0
96	More than one order enhancement in peak detectivity (D*) for quantum dot infrared photodetectors implanted with low energy light ions (Hâ^'). Applied Physics Letters, 2013, 102, 051105.	3.3	17
97	Proposed mechanism to represent the suppression of dark current density by four orders with low energy light ion (Hâ^') implantation in quaternary alloy-capped InAs/GaAs quantum dot infrared photodetectors. Materials Research Bulletin, 2013, 48, 2886-2891.	5.2	5
98	Comprehensive study on molecular beam epitaxy-grown InAs sub-monolayer quantum dots with different capping combinations. Journal of Vacuum Science and Technology B:Nanotechnology and Microelectronics, 2013, 31, 03C136.	1.2	11
99	Photoelectric Generation Coefficient of Bâ€Gallium Oxide during Exposure to Highâ€Energy Ionizing Radiation. Physica Status Solidi (A) Applications and Materials Science, 0, , 2100700.	1.8	0